A density functional theory study of CH 2 and H adsorption on Ni(111)

A. Michaelides and P. Hu

Citation: The Journal of Chemical Physics **112**, 6006 (2000); doi: 10.1063/1.481173
View online: http://dx.doi.org/10.1063/1.481173
View Table of Contents: http://scitation.aip.org/content/aip/journal/jcp/112/13?ver=pdfcov
Published by the AIP Publishing

A density functional theory study of CH_2 and H adsorption on Ni(111)

A. Michaelides and P. Hu[a)]
School of Chemistry, The Queen's University of Belfast, Belfast BT9 5AG, United Kingdom

(Received 16 August 1999; accepted 7 January 2000)

Ab initio total energy calculations within the density functional theory framework have been used to study the adsorption of CH_2 and H as well as the coadsorption of CH_2 and H on Ni(111). H binds strongly at threefold hollow sites with calculated adsorption energies of 2.60 and 2.54 eV at the face-centered-cubic (fcc) and hexagonal-close-packed (hcp) hollow sites, respectively. Adsorption energies and H-Ni distances are found to agree well with both experimental and theoretical results. CH_2 adsorbs strongly at all high symmetry sites with calculated adsorption energies of 3.26, 3.22, 3.14 and 2.36 eV at the fcc, hcp, bridge and top sites, respectively. Optimized structures are reported at all sites, and, in the most stable hollow sites there is considerable internal reorganization of the CH_2 fragment. The CH_2 molecule is tilted, the hydrogens are inequivalent and the C-H bonds are lengthened relative to the gas phase. In the CH_2-H coadsorption systems the adsorbates have a tendency to move toward bridge sites. The bonding of all adsorbates to the surface is analyzed in detail. © *2000 American Institute of Physics.* [S0021-9606(00)71213-X]

I. INTRODUCTION

The chemisorption and reaction of hydrogen and hydrocarbon fragments on catalytically active transition metal surfaces have been extensively studied due to the commercial importance of hydrocarbon formation reactions. CH_2 is the simplest member of the carbene homologous series. It has often been suggested that CH_2 is a reaction intermediate in many of the fundamental reactions in heterogeneous catalysis. In both the fuel reforming[1–4] and methanation[5–9] processes, for example, steps involving CH_2 and H have been suggested,

$$CH+2H \rightleftharpoons CH_2+H \rightleftharpoons CH_3.$$

In the fuel reforming process, CH_2 is produced after CH_4 dissociation and in the methanation reaction it is formed prior to CH_4. The first step in the quest to understand the above processes is to gain insight into how such reaction intermediates chemisorb upon the catalytic substrate. Once an understanding of the chemisorption has been reached, one can then look at how these adsorbates interact. In the present study we tackle both of these issues.

The adsorption of H on transition metal surfaces has been the subject of numerous investigations, and specific chemisorption systems, including H on Ni(111), have been well characterized.[10–21] H is found to bind quite strongly in fcc and hcp threefold hollow sites with no detectable difference in Ni-H bond lengths between the two sites.[11] The CH_2 adsorption system, on the other hand, is much more difficult to characterize experimentally. The difficulty in studying catalytic reaction intermediates, such as CH_2, is that they are short lived and concentrations are usually too small for spectroscopic identification. Numerous attempts to isolate and identify these species have been made. Kaminsky *et al.*[22] observed CH, CH_2 and CH_3 fragments in the methanation reaction of CO and H_2 on Ni(111) by secondary ion mass spectrometry (SIMS) and x-ray photoelectron spectroscopy (XPS). Demuth and Ibach[23] suggested that CH_2 may be present on Ni(111) after the decomposition of acetylene. Various precursors from which CH_2 can be more easily generated, for example dihaloalkanes (CH_2X_2), have been used on a wide variety of transition metals.[8,9] In these studies, CH_2 decomposition to surface C is found to be the dominant reaction pathway, although hydrogenation to methane has also been reported on several low index transition metal facets, Ni(111) being one of these.

In general, direct experimental determinations of the relative stabilities of CH_x fragments have proved elusive. Information on stabilities, therefore, has to be taken from theoretical calculations. Yang and Whitten have performed embedded cluster configuration interaction (CI) calculations for various adsorbates on Ni(111).[24] They have carried out a substantial part of the theoretical work for CH_x fragments on Ni(111)[25–27] and found that all CH_x fragments bind strongly at threefold and bridge sites. Adsorption energies, Ni-C bond lengths and C-H stretching frequencies were calculated. Yang and Whitten have also studied CH_x-H coadsorption systems and found that across-atom arrangements are the most stable. Siegbahn and Panas[28] have carried out bond prepared cluster calculations to model CH_x groups chemisorbed on Ni(100) and Ni(111). Calculated adsorption energies and optimized structures were given. Van Santen and co-workers[29–33] have carried out density functional calculations on methane activation and dehydrogenation in which the specific adsorption sites of CH_x fragments were discussed. Recently, Kua and Goddard,[34] as well as Paul and Sautet,[35] both using density functional methods, studied CH_x chemisorption on Pt(111) and Pd(111). Extended Huckel methods have also been widely used to study such systems. Chemisorption of hydrocarbon fragments on Ni(111) has

a)Author to whom correspondence should be addressed; electronic mail: p.hu@qub.ac.uk

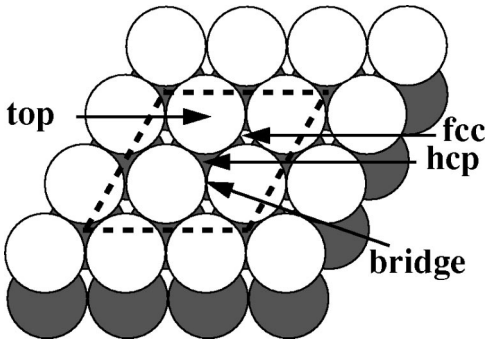

FIG. 1. A section of the Ni(111) surface. The arrows indicate the position of the four high symmetry adsorption sites. The dashed line represents the unit cell. Only two layers of metal atoms are shown for clarity.

been studied by Gavin *et al.*[36] Hoffmann and co-workers[37] have studied the bonding and coupling of CH_x groups on Co, Cr and Ti.

It has often been found that hydrocarbon adsorbates on transition metal surfaces exhibit an unusually ''soft'' C-H frequency.[38–43] Adsorbed CH_3 is one of the hydrocarbons that exhibits such a softened stretching frequency.[38] Recently, we have shown that for CH_3 this softened vibration is possibly associated with a C-H-Ni three-center bond.[44] In the present study we show that such three-center bonding interactions may also be present in the CH_2-Ni(111) adsorption system.

We present here spin polarized density functional theory calculations with gradient corrections for methylene and hydrogen as well as the methylene–hydrogen coadsorption system. The paper is organized as follows. Below, some of the details behind our total energy calculations are outlined. We report and discuss our results in Sec. III. In the first part of Sec. III, H chemisorption on Ni(111) is discussed. In the second part, methylene adsorption is considered. The third part deals with methylene–hydrogen coadsorption. The conclusions are outlined in the final section.

II. CALCULATIONS

Ab initio total energy calculations within the density functional theory (DFT) framework were carried out in this study.[45] The conjugate gradient minimization scheme was utilized to directly locate electronic ground states.[46] The basis set consists of plane waves. A Fermi smearing of 0.1 eV was utilized and the corrected energy extrapolated to zero Kelvin,[47] which considerably reduces **k**-point sampling. A spin polarized generalized gradient approximation (GGA)[48] was used throughout. A structure optimization of CH_2 in the gas phase was performed and the reference energy is taken to be CH_2 in the lowest energy triplet state, $^3B_1$.

Ab initio nonlocal pseudopotentials[49] of C, H and Ni in fully separable Kleinman-Bylander[50] form were used and it was found that a 550 eV cutoff was sufficient. The supercell approach was employed to model periodic geometries. Ni(111) was represented by three Ni layers fixed at bulk truncated positions. A $p(2\times2)$ unit cell was used (Fig. 1). In the individual chemisorption systems a single adsorbate was placed on one of the two surfaces, corresponding to a coverage of 0.25 of a monolayer. In the coadsorption systems, a single H as well as a single CH_2 were placed in the unit cell. A Monkhorst-Pack[51] mesh with $2\times2\times1$ **k**-grid sampling, in the surface Brillouin zone, was used.

TABLE I. A comparison between calculated and experimental bulk lattice constants of Ni. LDA is the Ceperly-Alder local density approximation. LSDA is the spin polarized version of the LDA, GGA refers to the spin-polarized version of the PW91 generalized gradient approximation.

	Expt.	LDA	LSDA	GGA
Lattice constant (Å)	3.5238	3.5323	3.5478	3.5122

We ensured that the properties of the isolated systems were accurately reproduced. Table I compares the calculated and experimental lattice constants of Ni. Table II compares the calculated and experimental[52,53] bond lengths and bond angles of some small molecules, including CH_2 and H_2. It is clear from Tables I and II that there is good agreement between calculated and experimental values. Tests concerning **k**-point sampling have also been performed: Structural parameters of the adsorption systems were converged, and energies were accurate to about 0.1 eV, with respect to an $8\times8\times1$ **k**-grid.

III. RESULTS AND DISCUSSION

A. H chemisorption on Ni(111)

The Ni(111) surface exhibits four high symmetry adsorption sites: top; bridge; and two threefold hollow sites, shown in Fig. 1. The threefold hollow sites differ only in their relationship with the second layer. The hcp threefold hollow site has a Ni atom directly below it, while the fcc threefold hollow site has a Ni atom only in the third layer. Both theoretical and experimental studies lead to the conclusion that hydrogen reactions with transition metals are exothermic, resulting in dissociation of H_2 and formation of strong H-metal bonds. With regard to H on Ni(111), it has been found that the threefold hollow sites are the most stable and thus these were the only sites investigated in this study. The chemisorption energies, E_{ads}, were calculated,

$$E_{\mathrm{ads}}=E_{\mathrm{Ni}}+E_{\mathrm{H}}-E_{\mathrm{H/Ni}},$$

where E_{Ni}, E_{H} and $E_{\mathrm{H/Ni}}$ are the total energies of Ni(111)-$p(2\times2)$, H and Ni(111)-$p(2\times2)$-H, respectively. H was found to bind quite strongly at both sites, with chemisorption energies of 2.60 and 2.54 eV at the fcc and hcp sites, respectively. Table III shows that these values agree with recent theory and experiment. A calculated H-H bond

TABLE II. A comparison between calculated and experimental structural parameters of free CH_2, CH_3, CH_4 and H_2.

	C-H (Å)		C-H angle (°)	
	Expt.	Calculated	Expt.	Calculated
CH_2	1.08	1.08	136	135.7
CH_3	1.08	1.08	120.0	120.0
CH_4	1.09	1.09	109.5	109.5
H_2	0.7414	0.7662	···	···

TABLE III. Adsorption energies and Ni-H bond lengths for the Ni(111)-$p(2\times2)$-H chemisorption system. Also shown for comparison are some recent theoretical and experimental results.

Site	E_{ads} (eV)	Ni-H (Å)
hcp[a]	2.54	1.75
fcc[a]	2.60	1.75
hcp[b]	2.69	1.86
fcc[b]	2.69	1.87
hcp[c]	2.91	1.70
fcc[c]	2.91	1.69
hollow	2.73[d]	1.84[d]

[a]This work.
[b]Yang and Whitten (Ref. 19).
[c]Paul and Sautet (Ref. 20).
[d]Christmann *et al.* (Ref. 10).

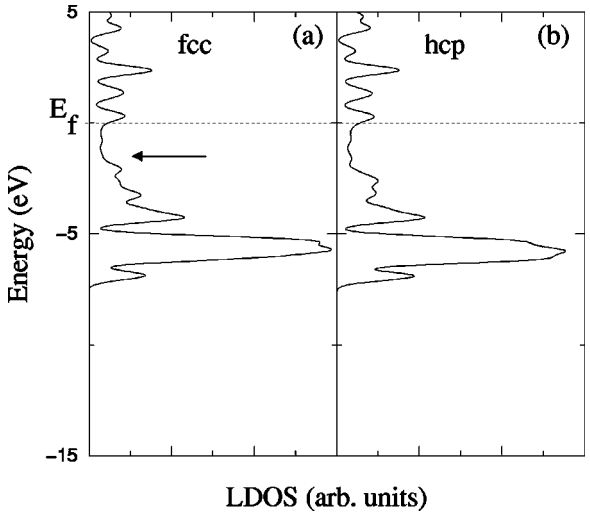

FIG. 2. Local density of states (LDOS) projected onto a 0.5 Å radius centered on H at the fcc and hcp sites. The Fermi levels have been aligned and set to 0 eV. The arrow indicates the center of the substrate density of states prior to adsorption.

energy of 4.45 eV yields an overall heat of reaction for $H_2(gas)\rightarrow 2H(ads)$ of 0.75 eV exothermic (not including vibrational zero point corrections). Experimentally[10] and theoretically[19] this value has been determined to be approximately 1 eV exothermic.

A H-Ni equilibrium bond length of 1.75 Å was found at both sites. The spin density of the Ni substrate decreases upon chemisorption. This agrees with previous work, which shows that the magnetic ordering of a Ni surface is reduced upon chemisorption of H.[54,55] Hydrogen gains charge upon adsorption. This has been determined by calculating the total number of electrons within spheres, of various radii, centered on H. Taking a 0.5 Å radius,[56] for example, upon adsorption the total number of electrons within this sphere increases from 0.277 to 0.373. This agrees with the CI calculations of Yang and Whitten.[19] They found that H gains 0.18 electrons upon adsorption.

The bonding of H to the Ni(111) surface has been analyzed using the local density of states (LDOS) and by examination of the real space distribution of individual quantum states. It is seen that the bonding characteristics are very similar at each of the threefold hollow sites. Figure 2 shows the LDOS projected onto H at the fcc and hcp threefold hollow sites. The dominant features at both sites are the hydrogen resonances at energies 7 to 4 eV below the Fermi level. The principal H level is 5.8 eV below E_F. This is in excellent agreement with the H feature seen in photoemission studies which also occurs at 5.8 eV below E_F.[16,17] States within this peak are principally H-1s Ni-3d bonding states. These findings are consistent with the calculations of Hammer and Nørskov.[21] Significant H-1s Ni-4s mixing is also observed, with the strongest mixing occurring at about 6 eV below E_F.

B. CH_2 Chemisorption on Ni(111)

1. Chemisorption energies

The energy of adsorption of CH_2 on Ni(111) has not been experimentally measured. Such a value is difficult to determine and requires very accurate calorimetric measurement. A theoretical approach is therefore useful. Yang and Whitten,[25] employing CI methods, have calculated chemisorption energies for each of the CH_x fragments. For CH_2 they obtained values of 2.91, 2.70, 2.72 and 1.58 eV for the hcp, fcc, bridge and top sites, respectively. Siegbahn and Panas[28] have performed multi-reference contracted configuration interaction (MRCCI) calculations and reported adsorption energies at the hollow (Ni_3) and top (Ni_{10}) sites of 3.82 and 3.12 eV, respectively. Using DFT cluster calculations, van Santen and co-workers[32] also found that CH_2 prefers hollow sites. Adsorption energies of 3.73, 2.75 and 2.92 eV at the hollow, bridge and top sites were reported. Clearly there are large discrepancies in the binding energies between these calculations. These differences are nontrivial since they have a bearing on how the CH_2 groups diffuse and react and ultimately on the stabilities of these fragments relative to the other CH_x intermediates. All of the above cluster calculations predict that the hollow sites are the most stable for CH_2 adsorption. On the other hand, extended Huckel calculations[37] found that on other transition metals, CH_x groups preferred to bind in such a way that C was in a tetrahedral environment. CH_3 was suggested to favor top sites, CH_2 bridge sites and CH hollow sites. Recently, two independent DFT studies[34,35] have had similar findings on Pt and Pd(111) surfaces. An older extended Huckel calculation on Ni(111)[36] did indeed find that the bridge site was the most stable chemisorption site for CH_2. We hoped that by performing periodic DFT calculations we might help to resolve these issues. To this end we carried out structure optimizations at the four high symmetry sites on the Ni(111) surface.

CH_2 is found to bind strongly at all four sites. Calculated chemisorption energies are 3.26, 3.22, 3.14 and 2.36 eV for adsorption at the hcp, fcc, bridge and top sites, respectively (Table IV). Clearly, the threefold hollow adsorption sites are the most stable with a difference of just 0.04 eV between them. The bridge site is only about 0.1 eV less stable, the top site is strongly disfavored by nearly 0.9 eV. The small difference between the threefold hollow and bridge sites indicates that the surface diffusion of CH_2 is quite easy.

Like H, CH_2 reduces the magnetic ordering of the substrate. CH_2 has a greater effect than H, and the magnitude of the reduction varies from site to site. We find that as the

TABLE IV. Adsorption energies for CH_2 adsorbed at the four high symmetry sites of Ni(111). At the bridge site, (a) and (b) refer to the two arrangements considered (Fig. 4).

Site	E_{ads} (eV)
fcc	3.26
hcp	3.22
bridge (a)	3.14
(b)	2.75
top	2.36

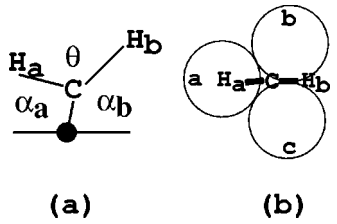

FIG. 3. Schematic structure of CH_2 adsorbed at a threefold hollow site. α_a and α_b are the surface-C-H_a and surface-C-H_b angles, respectively. (a) is viewed from the side. The horizontal line represents the center of the top layer of Ni atoms. The small black circle indicates the center of the threefold hollow site. (b) is viewed from above, the Ni surface is represented by circles.

chemisorption energy increases, the magnetic ordering of the underlying substrate decreases. Such relationships have been seen before.[57–59] A quantum state analysis shows that reduction is mainly localized in the atoms that bond directly to CH_2.

2. Structure of adsorbed CH_2

a. hcp and fcc threefold hollow sites. We begin by examining the most stable adsorption sites: the threefold hollow sites. Since the optimized structures obtained at both of these sites are very similar they will be discussed together.

First of all, it is constructive to consider the structure of free CH_2. CH_2 commonly occurs in two states, the low energy triplet ($^3B_1$) or the higher energy singlet ($^1A_1$). We calculated the structure of both states and found that the HCH angle (θ) was 136° in the triplet and 102° in the singlet. The equilibrium C-H bond lengths also differ, being 1.08 and 1.11 Å in $^3B_1$ and $^1A^1$, respectively.

Optimization at the threefold hollow sites of Ni(111) was performed by initially placing CH_2 at the center of each site, from where it was allowed to move in all directions to lower the total energy according to the forces calculated using the Hellmann-Feynman theorem. Upon adsorption at these sites, CH_2 undergoes considerable internal reorganization. Table V lists the final optimized structural parameters obtained at these and the other sites. Figure 3 shows the structure for CH_2 adsorbed at the hollow sites, in which the hydrogens have been arbitrarily labeled a and b. It can be seen clearly that the molecular fragment is tilted and the hydrogens are no longer equivalent. Considering the fcc site, for example, the C-H_a bond length is 1.11 Å and the C-H_b bond length is 1.10 Å. Both of these bonds are longer than the gas phase value of 1.08 Å for CH_2 in $^3B_1$ and closer to the C-H bond lengths of CH_2 in $^1A_1$. One explanation for why the C-H bond lengthens is that it does so as a consequence of being involved in a C-H-Ni three-center bond. We find that one of the C-H bonding orbitals in CH_2 mixes with Ni $3d$ states (also see Sec. III B 3). This mixing weakens the C-H bond and causes it to lengthen. The observation of lengthened C-H bonds is significant because it indicates that a softened mode similar to that observed for CH_3[38] may also be present for CH_2. Demuth and Ibach[39] who have obtained high-resolution electron energy-loss spectra (HREELS) for CH_2 on Ni(111) offer some indirect evidence for this. They assigned a peak at 1300 cm^{-1} to a perturbed scissors mode shifted to lower frequencies by a H-metal interaction. However, in the C-H stretching region of the spectra they reported that the signal to noise ratio was too poor to make a definitive interpretation of a softened mode. We believe that because the C-H-Ni interaction is greater in H_a than in H_b that two distinct C-H stretching vibrations, both of which are redshifted, should exist.

For CH_3 we have shown that the closer a H is to an underlying Ni, the longer its C-H bond would be.[44] This is also true for CH_2. At the hcp site, for example, the C-H_a bond is 1.12 Å and H_a is 2.03 Å from its nearest Ni neighbor. The C-H_b bond is 1.10 Å and H_b is 2.53 Å from its nearest Ni neighbor. The C of CH_2 is displaced from the center of the hollow site toward a bridge site: 0.15 and 0.11 Å at the fcc and hcp sites, respectively. When the C of the CH_2 group is fixed at the center of the hcp site the total energy is only 0.02 eV higher. Clearly the potential energy surface for CH_2 diffusion is very flat in this region.

b. bridge and top sites. During structure optimizations of CH_2 at these sites, the C atom was constrained to stay precisely above the ideal bridge and top positions, from where the rest of the molecule was allowed to relax. One calculation, at the bridge site, was performed, in which CH_2 was allowed to fully relax. In this case CH_2 moved away from the

TABLE V. Optimized structural parameters obtained for CH_2 adsorbed at the four high symmetry sites of Ni(111). C-$d_\perp$ is the C-surface perpendicular distance. θ is the H-C-H angle. At the hcp and fcc threefold sites H_a, H_b, Ni_a, Ni_b, Ni_c are as shown in Fig. 3. $\alpha_{a(b)}$ is the surface-C-$H_{a(b)}$ angle. At the bridge and top sites the hydogens and nickles are equivalent.

	C-H_a (Å)	C-H_b (Å)	C-Ni_a (Å)	C-Ni_b (Å)	C-Ni_c (Å)	C-$d_\perp$ (Å)	H_a-Ni_a (Å)	H_b-Ni_b (Å)	H_b-Ni_c (Å)	θ(°)	α_a(°)	α_b(°)
hcp	1.12	1.10	2.11	1.98	1.99	1.42	2.03	2.56	2.53	105.31	118.34	136.28
fcc	1.11	1.10	2.14	1.97	2.01	1.44	2.10	2.62	2.45	106.26	119.77	133.77
Bridge (a)	1.10		1.97			1.52	2.51			108.97		125.66
(b)	1.10		1.95			1.50	2.17			108.07		125.82
Top	1.09		1.85			1.85	2.59			113.10	123.37	

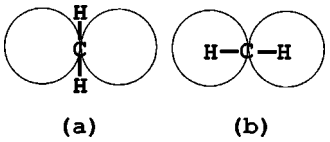

FIG. 4. Schematic structures of the two initial orientations of CH_2 adsorbed at the bridge site. (a) C is in a tetrahedral environment. (b) C is in a planar environment.

bridge into a three fold hollow site, again verifying that the threefold hollow sites are the most stable. Detailed structural parameters are listed in Table V. At both sites, unlike at the threefold hollow sites, the hydrogens of CH_2 are essentially equivalent and lie close to a horizontal plane.

Two initial orientations of CH_2 at the bridge site were tested and these are shown in Figs. 4(a) and 4(b). Upon optimization, it is found that configuration (a), which has *C* in a tetrahedral environment, is stable and the hydrogens, even when allowed to completely relax, stay close to the plane shown in Fig. 4(a). Configuration (b), however, which initially has *C* in a planar environment, is not stable. If the hydrogens of CH_2 in (b) are allowed to relax, they rotate by 90° into configuration (a). If the hydrogens of CH_2 are fixed in the plane of the bridge site, as indicated in Fig. 4(b), then this orientation is 0.39 eV less stable than structure (a). By contrasting the structure of CH_2 at the various sites, one can see that as the molecular fragment diffuses across the surface its internal structure changes.

3. Bonding

When analyzing the bonding of a methylene fragment to a metal surface it is beneficial to consider the orbitals of the methylene fragment itself. Knowledge of these orbitals allows us to predict, to a certain extent, how CH_2 is likely to bind to the underlying substrate. Two-dimensional electron density contour plots are displayed in Fig. 5 for the four occupied orbitals of free CH_2. CH_2 has C_{2V} symmetry and the orbitals are labeled accordingly. The $2a_1$ is the lowest energy orbital, then the $1b_1$ orbital followed by the $3a_1$ and $1b_2$ orbitals [Fig. 6(a)]. The $3a_1$ and $1b_2$ orbitals are both singly occupied in the $^3B_1$ state. Since the $3a_1$ and $1b_2$ orbitals are the highest occupied molecular orbitals of CH_2, and are partially occupied, one would expect that these would make the most substantial contribution to the CH_2-surface bond. The $2a_1$ and $1b_1$ orbitals, which reside at lower energies and are fully occupied, are expected to interact to a lesser extent. The bonding of CH_2 to Ni(111) is considered by a discussion of the most stable (threefold hollow) sites. Only a brief reference is made to the bridge and top sites.

a. hcp and fcc threefold hollow sites. Figure 6 shows the LDOS around carbon at each of the four sites. For comparison, the energies of the occupied orbitals of free CH_2 are also shown. By comparing the energy of the orbitals before and after chemisorption one can obtain a qualitative understanding of the changes that occur upon chemisorption. The larger the changes in energy that occur, the larger the interaction. It can be seen that the first peak (going from low to high energy) in Figs. 6(a) and 6(b) appears at slightly lower energy

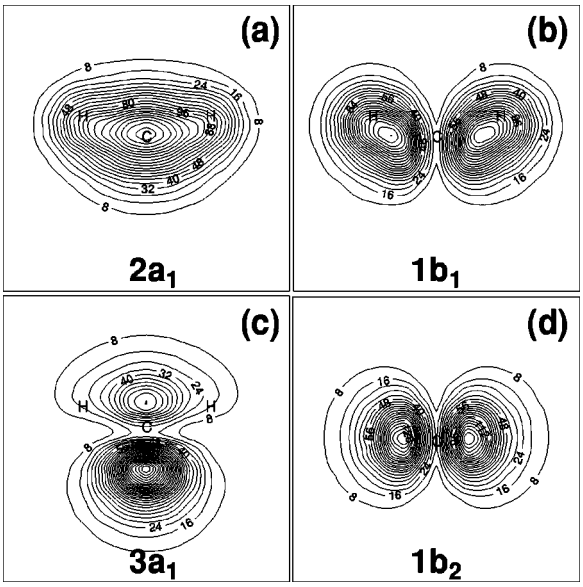

FIG. 5. Two-dimensional (2D) electron density contour plots for the four occupied orbitals of CH_2 in $^3B_1$. The plane of the cuts (a)–(c) is through the C-H-H nuclei. The plane of slice (d) is orthogonal to that used in (a)–(c). Density is in units of 3.63×10^{-3} electrons/bohr^3.

(about 1 eV) than the $2a_1$ orbital of free CH_2. By examining the real space distributions of the quantum states within this peak, we found that states within this peak do indeed contain strong $2a_1$ character. Figure 7(a) is a typical quantum state of this type. These states are relatively unchanged upon chemisorption. However, a very slight charge accumulation between *C* and the three surface atoms of the threefold hollow site was detected.

Within the second peak in Figs. 6(a) and 6(b) (about 7 eV below E_F) are states containing strong $1b_1$ character.

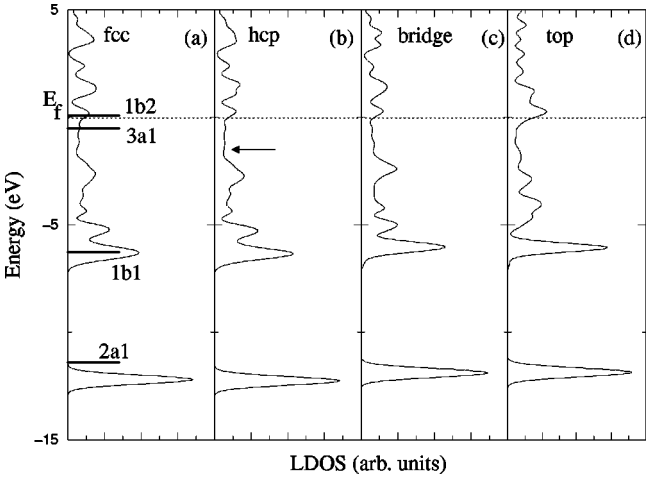

FIG. 6. Local density of states (LDOS) projected onto a 0.5 Å radius centered on *C* for CH_2 adsorbed at the four high symmetry sites of Ni(111). The Fermi levels have been aligned and set to 0 eV. This involves an average translation of the spectra in each graph by 4.90 eV. The straight horizontal lines represent the approximate energies of the four occupied orbitals of triplet CH_2. These energies were obtained by translating the eigenvalues of a free CH_2 by the average value (4.90 eV) that the chemisorption systems were translated by. The arrow in (b) indicates the center of the substrate density of states prior to adsorption.

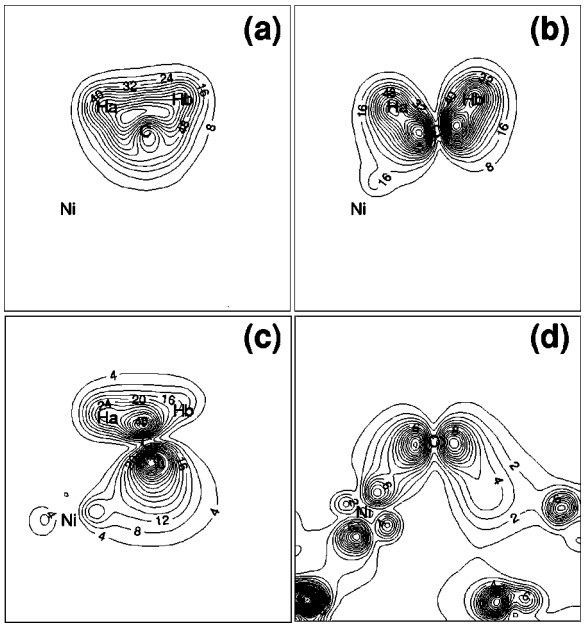

FIG. 7. 2D electron density contour plots of some typical quantum states for CH_2 adsorbed at the fcc threefold hollow site of Ni(111). The plane of the cuts (a)–(c) is through the C-H_a-Ni_a nuclei. The plane of slice (d) is orthogonal to that used in (a)–(c). Density is in units of 3.63×10^{-3} electrons/bohr^3.

These states occur at similar energies to the $1b_1$ orbital of the triplet state of free CH_2. A quantum state analysis, though, shows a slight mixing of the $1b_1$ orbitals with $3d$ orbitals of the surface Ni atoms, as shown in Fig. 7(b) for example. Such mixing would be expected to lower the kinetic energy of these eigenstates and so lower their energy, i.e., these states should reside at lower energies when CH_2 is chemisorbed at these sites. This anomaly can be explained as follows. Since the structure of chemisorbed CH_2 more closely resembles singlet CH_2, it is reasonable to compare the energy levels of the chemisorption systems to singlet CH_2. In singlet CH_2 the $1b_1$ orbital is more than 1 eV higher in energy than in triplet CH_2. Therefore, if the $1b_1$ level of singlet CH_2 is used as the energy reference these states are then shifted downward. There is no need to apply such an argument to the $2a_1$ derived states, as the difference in energy between the $2a_1$ orbitals in singlet and triplet CH_2 is not as large. This $1b_1$-$3d$ mixing is similar to the $1e_1$-$3d$ mixing detected in adsorbed CH_3 on Ni(111).[44] In CH_3 the C-H-Ni three center bonding can be clearly seen in the $1e_1 - 3d$ mixing states. Three-center bonding is an important factor that causes the C-H bonds of adsorbed CH_3 to lengthen, leading to the softened C-H stretching mode observed.

It is because of this $1b_1$-$3d$ mixing that the C-H bond lengths differ. The H_a-Ni bond is shorter than that of the H_b-Ni bond (Fig. 3). The portion of the $1b_1$ orbital centered on H_a mixes with the $3d$ orbitals of Ni_a [Fig. 7(b)]. Because of the greater H_b-Ni distance, the portion of the $1b_1$ orbital centered on H_b can not mix as strongly. This C-H-Ni mixing is in effect a charge transfer from the C-H bond toward the Ni. There is, therefore, more charge transfer from the C-H_a bond to Ni than that from the C-H_b bond. This can be verified by calculating the number of electrons around the two H atoms. Within a 0.5 Å radius[56] of both H nuclei, in gas phase CH_2, there are 0.482 electrons. In chemisorbed CH_2 at the fcc site, for example, there are 0.471 and 0.466 electrons around H_b and H_a, respectively. Clearly both hydrogens lose a small amount of charge upon adsorption, H_a losing more than H_b. The C-H_a bond is therefore weakened and lengthened more. It is obvious then that the hydrogens are inequivalent. Such inequivalence of the two hydrogens implies that when CH_2 dissociates one particular C-H bond will be more likely to break than the other.

$3a_1$-$3d$ mixing is observed within a broad energy continuum up to the Fermi level. The most pronounced bonding states are located within the third peak (about 6 eV below E_F) in Fig. 6. As a result of this mixing, charge accumulates between C and the three Ni atoms of the hollow site to produce a σ bond between CH_2 and the surface. A typical quantum state of this type is shown in Fig. 7(c). The energy of these orbitals decreases by up to 5 eV upon chemisorption compared to the $3a_1$ level of CH_2 in the gas phase. States of this type contribute the most to the CH_2-surface bond.

In the continuum of states above 5 eV below E_F, states of $1b_2$ character are also detected. The small peak at about 4 eV below E_F indicates the energy at which the greatest abundance of these states is observed. A typical quantum state of this type is shown in Fig. 7(d). Quite strong $1b_2$-$3d$ mixing is observed, although it is not as strong as $3a_1$-metal mixing and does not contribute as much to the CH_2-surface bond. This is evidenced by the higher average energies of the $1b_2$ derived states; they have not been shifted down in energy as much as the $3a_1$ derived states. The $1b_2$ orbital forms bonds with the surface which are π like in character. The $3a_1$ orbital, on the other hand, forms bonds with greater σ character to the surface. Hoffmann and co-workers,[37] who have studied CH_2 adsorption on Ti, Cr and Co, have had similar findings regarding the overlap of the $3a_1$ and $1b_2$ orbitals with the underlying surface.

b. bridge and top sites. There is an increase in energy in most of the molecularly derived states at these sites compared to the threefold hollow sites. At the bridge site this energy increase is slight [Fig. 6(c)] and at the top [Fig. 6(d)] it is more dramatic. At the top site, states of $3a_1$ character are pushed up considerably and little $1b_2$ metal mixing is observed.

C. Coadsorption of CH_2 and H

After an understanding of the individual chemisorption systems has been established, the next issue one can tackle is to see how the individual species interact when they are coadsorbed. Five coadsorption arrangements were studied, all of which have CH_2 and H initially adsorbed at hcp and fcc threefold hollow sites. Figure 8 shows the initial arrangements of each of the coadsorption systems. The adsorbates were initially placed at their equilibrium positions as determined from their individual chemisorption (Secs. III A and III B 2), within the same unit cell. Both CH_2 and H were then allowed to relax completely. The total chemisorption energies of the coadsorption systems were then compared to the

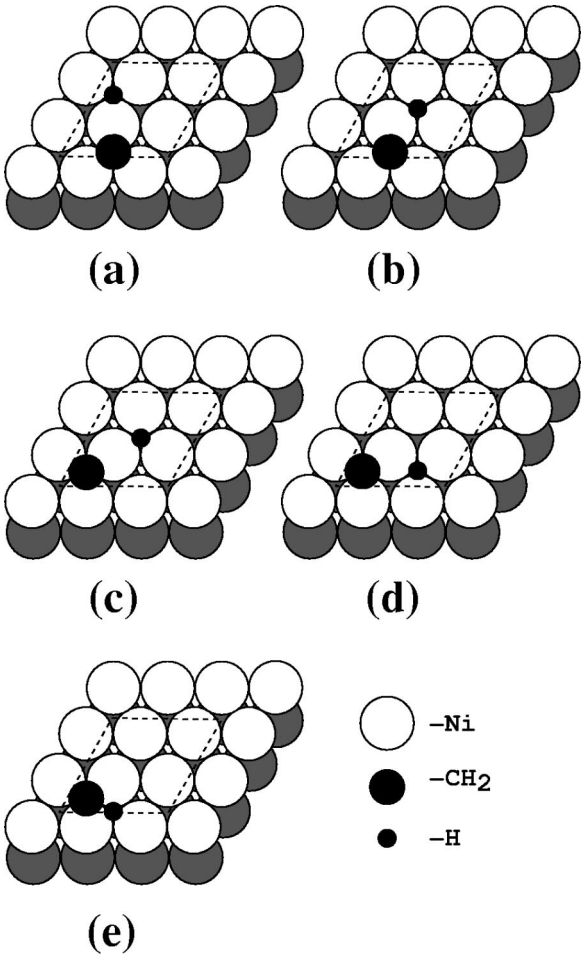

FIG. 8. The five CH_2/H coadsorption systems calculated. For clarity, the periodic nature of the systems is not shown.

sum of the individual CH_2 and H chemisorption energies. The total chemisorption energies of each coadsorption system, with the exception of structure (*e*) which was not stable,[60] were found to be only slightly lower than the sum of the individual chemisorption energies. The most stable arrangement identified is structure (*c*), in which CH_2 and H are initially adsorbed at fcc and hcp sites, respectively. This arrangement is 0.10 eV lower in total chemisorption energy than the sum of the chemisorption energies when CH_2 and H are chemisorbed in individual unit cells. The next most stable arrangement, shown in Fig. 5(d), is 0.18 eV lower in total chemisorption energy than the individual chemisorption of CH_2 and H. In this arrangement, CH_2 is again initially

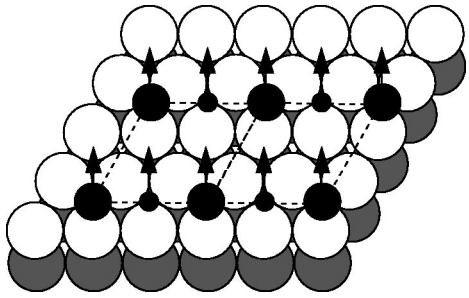

FIG. 9. Schematic diagram indicating the direction in which the adsorbates move upon optimization. H (small black circles) moves more than CH_2 (large black circles).

adsorbed at an fcc site with H also adsorbed at an fcc site. Configurations (a) and (b) which initially have hcp-fcc and hcp-hcp arrangements of CH_2 and H are 0.21 and 0.24 eV, respectively, lower in total chemisorption energy than separate chemisorption. Yang and Whitten[26] have calculated some CH_2 and H coadsorption situations on Ni(111). They also found that it costs energy to bring CH_2 and H together, although they reported that arrangement (b) (hcp-hcp arrangement of CH_2 and H), for example, was much lower in total chemisorption energy (1.36 eV) relative to separate chemisorption of CH_2 and H.

The optimized structures for the four stable arrangements are listed in Table VI. In each system, especially (b) and (d), a small yet very interesting movement of the adsorbates has been detected. H, and to a lesser extent CH_2, move away from their initial positions toward bridge sites (Fig. 9). Considering structure (d), for example, both H and CH_2 move 0.16 and 0.08 Å, respectively, toward their neighboring bridge sites in the coadsorption system compared to their preferred positions when chemisorbed in separate unit cells. Figure 9 indicates that when the adsorbates move toward bridge sites they always move toward the same row of Ni atoms.

This contravenes bonding competition[61,62] or least atom sharing models of coadsorption. Usually when species adsorb they prefer to share bonding to surface atoms with the least number of other adsorbates. In the structure optimizations, initially CH_2 and H are placed within the same unit cell at their equilibrium positions as for pure CH_2 and pure H chemisorption. At these positions the adsorbates bond nearly equally to each of the three atoms of their respective fcc hollow sites. Each adsorbate shares two of its three surface atoms with the other, and has one surface atom to which it alone is bonded. Upon optimization, one would expect that

TABLE VI. Optimized structural parameters for the four stable CH_2/H coadsorption systems. H(ads)-$d_\perp$ and C-$d_\perp$ refer to the adsorbed H-surface and C-surface perpendicular distances, respectively. θ is the H-C-H angle and $\alpha_{a(b)}$ is the surface-C-$H_{a(b)}$ angle. H(ads)-Ni and C-Ni refer to the shortest H-Ni/C-Ni distance of each coadsorption system.

	H(ads)-Ni (Å)	H(ads)-$d_\perp$ (Å)	C-H_a (Å)	C-H_b (Å)	C-Ni (Å)	C-$d_\perp$ (Å)	θ(SD)	α_a(°)	α_b(°)
(a)	1.69	1.00	1.12	1.10	1.97	1.42	103.67	115.01	141.30
(b)	1.67	0.97	1.12	1.09	1.98	1.44	104.38	115.16	140.34
(c)	1.70	0.96	1.11	1.09	1.97	1.43	105.55	118.27	136.02
(d)	1.69	0.98	1.12	1.09	1.97	1.42	105.07	118.27	136.65

the adsorbates would try to share bonding with the least number of surface atoms. Exactly the opposite behavior is observed: Both adsorbates move toward the same row of Ni atoms (Fig. 9). As a consequence, there are other rows of Ni atoms which are more weakly bonded to the adsorbates than others. We must stress that this effect is very subtle, as the energetic difference between the initial (CH_2 and H at their equilibrium positions within the same unit cell as determined from their individual chemisorption) and optimized structures is only about 0.05 eV in each coadsorption system.

In order to understand this further we performed the following calculations. First, CH_2 was replaced with H in coadsorption arrangement (a) of Fig. 8. No movement toward bridge sites was found. Second, CH_2 was replaced with CH_3. Again, no movement toward bridge sites was detected. Clearly then this effect is a consequence of CH_2. The bonding within the coadsorption systems has been analyzed in detail. It has proved difficult, as yet, to ascertain an explanation for this movement. One observation, though, which stands out, is that the density around the chemisorbed H increases upon relaxation. Considering arrangement (d) in Fig. 8, for example, the total valence electron count around H both prior to and after relaxation has been calculated and this has been compared to the total number of valence electrons around H for pure H chemisorption. For pure H chemisorption, at the fcc site, 0.373 electrons are located within a radius of 0.5 Å. Before optimization in coadsorption system (d) there are only 0.367 electrons within this radius. After optimization the optimum value of 0.373 electrons within a 0.5 Å radius is again observed.

IV. CONCLUSIONS

H binds strongly at threefold hollow sites with calculated adsorption energies of 2.60 and 2.54 eV at the fcc and hcp hollow sites, respectively. Adsorption energies and H-Ni distance are found to agree well with both experimental and theoretical results. The main H-Ni bond is a H $1s$-Ni-$3d$ mixing which occurs 5.8 eV below the Fermi level. CH_2 adsorbs strongly at all high symmetry sites with calculated adsorption energies of 3.26, 3.22, 3.14 and 2.36 eV at the fcc, hcp, bridge and top sites, respectively. It is expected that the surface diffusion of CH_2 from hollow sites via bridge sites is quite easy. Optimized structures are reported and found to differ at all sites. Consequently, as CH_2 diffuses across the surface its internal structure changes. In the most stable hollow sites there is considerable internal reorganization of the CH_2 fragment. The CH_2 molecule is tilted and the hydrogens are inequivalent. As was the case for CH_3 adsorbed on Ni(111), C-H-Ni three-center bonding has been detected. The bonding of CH_2 to the Ni surface is characterized by weak $2a_1$ and $1b_1$ metal mixing. Very strong $3a_1$-metal mixing resulted in a σ type bond with the surface. $1b_2$-metal mixing is also strong. In the CH_2-H coadsorption systems the adsorbates have a tendency to move toward bridge sites.

ACKNOWLEDGMENTS

The Supercomputing Center for Ireland is gratefully acknowledged for computer time and the authors wish to thank EPSRC for their financial support.

[1] F. Besenbacher, I. Chorkendorff, B. S. Clausen, B. Hammer, A. M. Molenbroek, J. K. Nørskov, and I. Stensgaard, Science **279**, 1913 (1998).
[2] J. P. Van Hook, Catal. Rev. Sci. Eng. **21**, 1 (1980).
[3] Rostrup-Nielson, *Catalysis-Science and Technology*, edited by J. R. Anderson and M. Boudert (Springer-Verlag, Berlin, 1984), Vol. 5, p. 1.
[4] P. Kratzer, B. Hammer, and J. K. Nørskov, J. Chem. Phys. **105**, 5595 (1996).
[5] A. Michaelides, P. Hu, and A. Alavi, J. Chem. Phys. **111**, 1343 (1999).
[6] A. D. Johnson, S. P. Daly, A. L. Utz, and S. T. Ceyer, Science **257**, 233 (1992).
[7] J. T. Yates, Jr., S. M. Gates, and J. N. Russell, Jr., Surf. Sci. **164**, L839 (1985).
[8] B. E. Bent, Chem. Rev. **96**, 1361 (1996).
[9] F. Zaera, Chem. Rev. **95**, 2651 (1995).
[10] K. Christmann, O. Schober, G. Ertl, and M. Neumann, J. Chem. Phys. **60**, 4528 (1974).
[11] K. Christmann, R. J. Behm, G. Ertl, M. A. van Hove, and W. H. Weinberg, J. Chem. Phys. **70**, 4168 (1979).
[12] A. Winkler, Appl. Phys. A: Mater. Sci. Process. **67**, 637 (1998).
[13] J. Boh, G. Eilmsteiner, K. D. Rendulic, and A. Winkler, Surf. Sci. **395**, 98 (1998).
[14] K. Mortenson, F. Besenbacher, I. Stensgaard, and W. R. Wampler, Surf. Sci. **205**, 433 (1988).
[15] W. Ho, N. J. DiNardo, and E. W. Plummer, J. Vac. Sci. Technol. **17**, 314 (1980).
[16] J. E. Demuth, Surf. Sci. **65**, 369 (1977).
[17] H. Conrad, G. Ertl, J. Kuppers, and E. E. Latta, Surf. Sci. **58**, 578 (1976).
[18] H. Yang and J. L. Whitten, Surf. Sci. **370**, 136 (1997).
[19] H. Yang and J. L. Whitten, J. Chem. Phys. **98**, 5039 (1993).
[20] J.-F. Paul and P. Sautet, Surf. Sci. **356**, L403 (1996).
[21] B. Hammer and J. K. Nørskov, Nature (London) **376**, 238 (1995).
[22] M. P. Kaminsky, N. Winograd, G. L. Geoffroy, and M. A. Vannice, J. Am. Chem. Soc. **108**, 1315 (1986).
[23] J. E. Demuth and H. Ibach, Surf. Sci. **78**, L238 (1978).
[24] J. L. Whitten and H. Yang, Surf. Sci. Rep. **218**, 55 (1996).
[25] H. Yang and J. L. Whitten, Surf. Sci. **255**, 193 (1991).
[26] H. Yang and J. L. Whitten, J. Am. Chem. Soc. **113**, 6442 (1991).
[27] H. Yang and J. L. Whitten, J. Chem. Phys. **91**, 126 (1989).
[28] P. Siegbahn and I. Panas, Surf. Sci. **240**, 37 (1990).
[29] H. Burghgraef, A. P. J. Jansen, and R. A. van Santen, J. Chem. Phys. **98**, 8810 (1993).
[30] H. Burghgraef, A. P. J. Jansen, and R. A. van Santen, Chem. Phys. **177**, 407 (1993).
[31] H. Burghgraef, A. P. J. Jansen, and R. A. van Santen, J. Chem. Phys. **101**, 11012 (1994).
[32] H. Burghgraef, A. P. J. Jansen, and R. A. van Santen, Surf. Sci. **324**, 345 (1995).
[33] A. D. Koster and R. A. van Santen, J. Catal. **127**, 141 (1991).
[34] J. Kua and W. A. Goddard III, J. Phys. Chem. B **102**, 9481 (1999); **102**, 9492 (1999).
[35] J.-F. Paul and P. Sautet, J. Phys. Chem. B **102**, 1578 (1998).
[36] R. M. Gavin, J. Reutt, and E. L. Muetterties, Proc. Natl. Acad. Sci. USA **78**, 3981 (1981).
[37] C. Zheng, Y. Apeloig, and R. Hoffmann, J. Am. Chem. Soc. **110**, 749 (1988).
[38] Q. Y. Yang, K. J. Maynard, A. D. Johnson, and S. T. Ceyer, J. Chem. Phys. **102**, 7734 (1995).
[39] J. E. Demuth, H. Ibach, and S. Lehwald, Phys. Rev. Lett. **40**, 1044 (1978).
[40] M. A. Chesters, S. F. Parker, and R. Raval, J. Electron Spectrosc. Relat. Phenom. **39**, 155 (1986).
[41] R. Raval and M. A. Chesters, Surf. Sci. **219**, L505 (1989).
[42] E. Cooper, A. M. Coats, and R. Raval, J. Chem. Soc., Faraday Trans. **91**, 3703 (1995).
[43] J.-L. Lin and B. E. Bent, Chem. Phys. Lett. **194**, 208 (1992).
[44] A. Michaelides and P. Hu, Surf. Sci. **437**, 362 (1999).
[45] P. Hu, D. A. King, S. Crampin, M. H. Lee, and M. C. Payne, Chem. Phys.

Lett. **230**, 501 (1994); P. Hu, D. A. King, M. H. Lee, and M. C. Payne, *ibid.* **246**, 73 (1995).
[46] M. C. Payne, M. P. Teter, D. C. Allen, T. A. Arias, and J. D. Joannopolous, Rev. Mod. Phys. **64**, 1045 (1992), and references therein.
[47] M. J. Gillan, J. Phys.: Condens. Matter **1**, 689 (1989).
[48] J. P. Perdew, J. A. Chevary, S. H. Vosko, K. A. Jackson, M. R. Pederson, D. J. Singh, and C. Fiolhais, Phys. Rev. B **46**, 6671 (1992).
[49] J.-S. Lin, A. Qteish, M. C. Payne, and V. Heine, Phys. Rev. B **47**, 4174 (1993).
[50] L. Kleinman and D. M. Bylander, Phys. Rev. Lett. **48**, 1425 (1982).
[51] H. J. Monkhorst and J. D. Pack, Phys. Rev. B **13**, 5188 (1976).
[52] *Handbook of Chemistry and Physics*, 80th ed., edited by D. R. Lide (CRC, London, 1999).
[53] E. Wasserman, Chem. Phys. Lett. **24**, 18 (1974).
[54] F. Mele, N. Russo, and M. Toscano, Surf. Sci. **251**, 46 (1991).
[55] M. Weinert and J. W. Davenport, Phys. Rev. Lett. **54**, 1547 (1985).
[56] The choice of radius is quite arbitrary, the same behavior is observed at various radii.
[57] P. D. Johnson, J. Electron Spectrosc. Relat. Phenom. **51**, 249 (1990).
[58] P. W. Selwood, *Chemisorption and Magnetization* (Academic, New York, 1975).
[59] R. Fournier and D. R. Salahub, Surf. Sci. **238**, 330 (1990).
[60] The C-H_{ads} distance was so short that upon optimization CH_2 and H coupled to produce CH_3.
[61] A. Alavi, P. Hu, T. Deutsch, P. L. Silvestrelli, and J. Hutter, Phys. Rev. Lett. **80**, 3650 (1998).
[62] K. Bleakley and P. Hu, J. Am. Chem. Soc. **121**, 7644 (1999).